RSC Advances

ROYAL SOCIETY OF CHEMISTRY

www.rsc.org/advances

Sandwich-like graphene nanosheets decorated with superparamagnetic $CoFe_2O_4$ nanocrystals and its applications as enhanced electromagnetic wave absorber

Xinghua Li[a, 1, *], Juan Feng[b, 1], Hao Zhu[c, 1], Chunhao Qu[d], Jintao Bai[a, e], Xinliang Zheng[a, *]

[a] Department of Physics, Northwest University, Xi'an 710069, China

[b] Key Laboratory of Magnetism and Magnetic Materials of Ministry of Education, School of Physical Science and Technology, Lanzhou University, Lanzhou 730000, China

[c] College of Chemistry and Chemical Engineering, Lanzhou University, Lanzhou 730000, China

[d] Shaanxi Research Design Institute of Petroleum and Chemical Industry, Xi'an 710069, China

[e] Institute of Photonics and Photo-Technology, Provinical Key Laboratory of Photoelectronic Technology, Northwest University, Xi'an 710069, China

[1] These authors contributed equally to this work

*Corresponding authors: Xinghua Li (lixinghua04@gmail.com) and Xinliang Zheng (zhengxl@nwu.edu.cn)

Abstract

Sandwich-structured $CoFe_2O_4$/graphene hybrids are fabricated through a facile one-pot polylol route, and the electromagnetic wave absorption properties are investigated. TEM images and element mapping indicate that the graphene nanosheets are decorated with numerous tiny $CoFe_2O_4$ nanocrystals with relatively uniform size of 7.2 nm, forming sandwich-like nanostructures. Magnetization measurement reveals that the $CoFe_2O_4$/graphene hybrids possess superparamagnetism at room temperature with zero coercivity. Investigations of the electromagnetic properties indicate that the complex permittivity of $CoFe_2O_4$/graphene hybrids is significantly improved in comparison with that of pure $CoFe_2O_4$ nanocrystals, leading to enhanced electromagnetic wave absorption properties of the $CoFe_2O_4$/graphene hybrids. The maximum reflection loss for the $CoFe_2O_4$/graphene hybrids is up to -36.4 dB at 12.9 GHz with the matching thickness of 2.5 mm, and the absorption bandwidth with the reflection loss values below -10 dB is in the ranges of 5.4-18 GHz when the matching thicknesses are only 1.5-4.0 mm. These results suggest that the sandwich-like $CoFe_2O_4$/graphene hybrids with enhanced electromagnetic wave absorption properties and wide absorption bandwidth are proposed to ideal candidate for electromagnetic wave absorption applications in the future.

Keywords: $CoFe_2O_4$, graphene, sandwich-like nanostructures, magnetic properties, electromagnetic wave absorption.

1. Introduction

During the past few years, the phenomenon of electromagnetic interference (EMI) and

electromagnetic compatibility (EMC) has become a serious problem, owing to the ever-increasing development of telecommunications and electronic devices working in gigahertz (GHz) range.[1-3] The accompanying electromagnetic pollution can not only interrupt the operation of electronic devices but also is harmful to human health, which causes the necessity for the electromagnetic interference shielding. Electromagnetic wave absorbing materials have drawn tremendous attention in fields of wireless devices, industrial protection and military, owing to that they can absorb the electromagnetic wave and convert them into thermal energy or dissipate them by the interference.[4,5] The electromagnetic wave absorbing materials with strong adsorption value, wide adsorption frequency, thin matching thickness and light weight are intensively requested.[5,6] Much effort has been focused on the fabrication of electromagnetic wave absorbing materials, such as ferrites, magnetic metals, dielectrics and so on.[7-10] However, the large density and high matching thickness of these materials greatly restricts their technical applications. The exploration of high efficient electromagnetic wave absorbing materials with light weight and thin thickness is still a big challenge.

Nowadays, graphene has attracted many scientific interests both in the fundamentally theoretical and experimental scientific research because of its remarkable chemical, physical and mechanical properties.[11] The high dielectric loss and low density make graphene a promising material for electromagnetic wave absorption properties. However, the maximum reflection loss of graphene is only -6.9 dB,[12] which is unsuitable for practical applications. Owing to its large surface area

and special layered structure, graphene has been promised to be nanoscale building blocks for novel hybrid materials.[13-16] Recently, decorating graphene nanosheets with magnetic nanoparticles, such as Fe_3O_4,[4,5] $NiFe_2O_4$,[17,18] Co_3O_4,[19,20] Fe,[21,22] Ni[23], γ-Fe_2O_3,[24] etc., has been widely applied for electromagnetic wave absorption, which is possibly resulted from the synergistic effect of their high magnetic loss from magnetic nanomaterials and electric loss from light-weight graphene, leading to well impedance matching and high-performance electromagnetic wave attenuation. However, the low loading density of magnetic nanoparticles on the graphene nanosheets makes the complex permeability of the hybrids hard to improve, which possibly limits the electromagnetic wave-absorbing applications of these hybrids. To our best knowledge, few papers have been reported on the fabrication of sandwich-like graphene-based hybrids with large coverage density for electromagnetic wave absorption applications.

Magnetic $CoFe_2O_4$ spinel ferrite has large saturation magnetization, large magnetocrystalline anisotropy and high Snoek's limit, which is promised to have high complex permeability in a wide frequency range. These characteristics suggest that $CoFe_2O_4$ can be used as thin electromagnetic wave absorbers working at high frequency range.[25,26] However, the large density of $CoFe_2O_4$ make it useless in the applications requiring lightweight mass.[26] In addition, the $CoFe_2O_4$ nanocrystals reported before shows large coercivity, which restricts their applications in high frequency. Recently, novel $CoFe_2O_4$-based electromagnetic wave absorption materials have been investigated, such as CNTs/$CoFe_2O_4$,[25] ZnO/$CoFe_2O_4$[26] and

polyaniline/$CoFe_2O_4$.[27] Furthermore, $CoFe_2O_4$/graphene hybrids have been used for microwave absorption applications, which were fabricatied through hydrothermal route in combination with annealing treatment or adjusting the reaction parameters.[28,29] However, these reported hydrothermal route is energy-intensive and needs rigorous reaction condition, which may hinder their industrial applications. Besides, it is still a big chanllege to fabricate large area of graphene nanosheets uniformly decorated by magnetic nanocrystals without aggregation. To our best knowledge, No paper has been focused on the fabrication of sandwich-like graphene nanosheets decorated with superparamagnetic $CoFe_2O_4$ nanocrystals for electromagnetic wave-absorbing applications.

In this paper, sandwich-like graphene nanosheets decorated with superparamagnetic $CoFe_2O_4$ nanocrystals was fabricated by a facile one-pot polyol route. The structure and morphology was characterized at nanoscale. Electromagnetic wave absorption investigations showed that the sandwich-structured superparamagnetic $CoFe_2O_4$/graphene hybrids exhibited excellent electromagnetic wave absorbability than pure graphene and $CoFe_2O_4$ nanocrystals. The results indicate that the sandwich-structured $CoFe_2O_4$/graphene hybrids are ideal candidate for future electromagnetic wave absorption applications.

2. Experimental section

2.1 Synthesis of sandwich-structured $CoFe_2O_4$/graphene hybrids

Graphene oxide (GO) was prepared through a modified Hummers method.[30] The sandwich-structured $CoFe_2O_4$/graphene hybrids were synthesized by an one-pot

polyol method. In a typical procedure, 40 mg GO was dispersed into 100 ml of ethylene glycol (EG) and ultrasounded for 3 h. 8 mmol $FeCl_3 \cdot 6H_2O$ and 4 mmol $CoCl_2 \cdot 6H_2O$ were added into the above suspension of GO and ultrasounded for another 3 h. 60 mmol NaAc was dissolved into the above solution. The solution was stirred and refluxed for 10 h. The black products were washed by water and ethanol for several times, and then dried in the atmospheric environment. For comparison purposes, pure $CoFe_2O_4$ nanocrystals were fabricated in the same approach without GO.

2.2 Characterization

The morphology and microstructure of the products were observed by high-resolution transmission electron microscope (HRTEM, FEI Tecnal G^2 F20) embedded with energy-dispersive X-Ray spectroscopy (EDX, Oxford Instrument), high angle annular dark field (HAADF) and scanning transmission electron microscopy (STEM). The crystal structure were performed by X-ray powder diffraction instrument with Cu K_α radiation (λ=1.5418 Å) (XRD, X'pert powder, Philips). The surface composition and oxidation state was obtained by the X-ray photoelectron spectroscopy (XPS, ESCALAB210). The magnetic properties were studied by vibrating sample magnetometer (VSM, Lake Shore 7,304). The electromagnetic parameters were analyzed by a network analyzer (Agilent Technologies E8363B), in which the powders were mixed with paraffin with 70 wt% samples and pressed into toroidal shape (ψ_{out}: 7.00 mm, ψ_{in}: 3.04 mm).

3. Results and Discussion

Fig. 1 shows the XRD patterns of GO and $CoFe_2O_4$/graphene hybrids. GO exhibits a strong diffraction peak at 13.4 °, corresponding to the (001) reflection with an interlayer spacing of 0.65 nm, which is larger than that of graphite (0.34 nm). The enhancement of interlayer spacing is due to the formation of oxygenic functional groups between the graphite layers.[31] For the $CoFe_2O_4$/graphene hybrids, the diffraction peaks at 2θ=30.1 °, 35.3 °, 43.1 °, 53.2 °, 56.9 °, 62.4 ° and 74.3 ° can be respectively indexed to the (220), (311), (400), (422), (511), (440) and (533) crystal planes of the pure spinel $CoFe_2O_4$ with a face-centered cubic (FCC) structure (Fd-3m, JCPDS card NO. 22-1086), suggesting the formation of $CoFe_2O_4$ nanocrystals. It is clear that the $CoFe_2O_4$/graphene hybrids show broadening diffraction peaks, suggesting that the crystalline grain is small. Based on the Scherer's formula, the average grain size of the $CoFe_2O_4$ nanocrystals is about 4.2 nm.

The morphologies of GO and $CoFe_2O_4$/graphene hybrids were characterized by TEM observations (Fig. 2). The layered GO (Fig. 2a and b) was transparent with several wrinkles at the edges. The SAED pattern of GO (inset of Fig. 2a) shows a set of six fold patterns, indicating that GO is few-layer with a hexagonal closed-packed (hcp) structure.[31] HRTEM image (inset of Fig. 2b) indicates that each GO nanosheet is about 3 layers. Fig. 2c-f show the TEM images of the $CoFe_2O_4$/graphene hybrids with different magnification. It is clearly seen that tiny $CoFe_2O_4$ nanocrystals with diameters of 7.8 nm covered evenly on the whole surface of graphene, forming sandwich-like structures. The SAED pattern of $CoFe_2O_4$/graphene hybrids (inset of Fig. 1c) shows the standard ring patterns resulted from the cubic spinel structure of

$CoFe_2O_4$, which is consistent with the XRD result. The HRTEM image of $CoFe_2O_4$ nanocrystals (inset of Fig. 2d) shows clear lattice fringes with a interplanar distance of 0.297 nm, which can be assigned to the (220) plane of $CoFe_2O_4$.

The chemical composition of the samples was characterized by XPS spectra (Fig. 3). In the full scan XPS spectrum (Fig. 3a), several sharp peaks with the binding energy of 285, 530, 711 and 790 eV, were attributed to C 1s, O 1s, Fe 2p and Co 2p, respectively, indicating the existence of C, O, Fe and Co elements in the $CoFe_2O_4$/graphene hybrids. To further investigate the electronic states of the elements for the samples, high-resolution spectra were analyzed. In the O 1s spectrum (Fig. 3b), the intensity of oxygen peak for $CoFe_2O_4$/graphene hybrids was visibly reduced in comparison with that of GO, revealing that the oxygen-containing groups in $CoFe_2O_4$/graphene hybrids is partly removed. Besides, the binding energy associated with O 1s shifted from 532.6 eV in GO to 530.4 eV in $CoFe_2O_4$/graphene hybrids, which is originated from the lattice oxygen in M-O (M=Fe, Co). The Fe 2p spectrum (Fig. 3c) exhibits two peaks at 712.23 and 725.62 eV, corresponding to $Fe2p_{3/2}$ and $Fe2p_{1/2}$, respectively. The Co 2p spectrum (Fig. 3d) consist of two spin-orbit doublets characteristics of $Co2p_{3/2}$ (778.6 eV, Co^{2+} in octahedron site; 784.2 eV, Co^{2+} in tetrahedron site) and $Co2p_{1/2}$ (794.0 eV, Co^{2+} in octahedron site; 800.8 eV, Co^{2+} in tetrahedron site). These results suggest the formation of $CoFe_2O_4$ nanocrystals. The C 1s spectrum of GO (Fig. 3e) consist of four deconvoluted peaks, arising from the C-C/C=C (285.0 eV), C-OH (286.1 eV), C-O-C (287.1 eV) and C=O (288.9 eV) groups. For the C 1s spectrum of $CoFe_2O_4$/graphene hybrids (Fig. 3f), the peak is

mainly the non-oxygenated carbon groups (C-C/C=C) and the relative contribution of oxygenated functional groups (C-O-C/C=O) decreased obviously, suggesting that most of the oxygenated functional groups were partly removed during the reaction process. The area ratios of the deconvoluted peaks for carbon-based functional groups of GO and $CoFe_2O_4$/graphene hybrids are displayed in Table 1. The XPS results further indicate that GO was reduced, during which $CoFe_2O_4$ nanocrystals were formed and anchored on the graphene nanosheets. The reduction of GO could significantly improve the electronic conductivity of $CoFe_2O_4$/graphene hybrids, making the graphene nanosheets as conductive channels between $CoFe_2O_4$ nanocrystals, which is favorable for electromagnetic wave absorption applications.[32]

To further determine the situation of $CoFe_2O_4$ nanocrystals supported on graphene, HAADF-STEM and EDX elemental mapping techniques were used to investigate the morphology and element distributions of $CoFe_2O_4$/graphene hybrids. HAADF-STEM images, called *Z*-contrast images (*Z* is the atomic number), make it ideal and powerful for the characterization of heterogeneous nanocomposites with components of different atomic numbers.[33] It is believed that this *Z*-contrast images could offer a better distinction between $CoFe_2O_4$ (average $Z \approx 16$) and C ($Z = 6$). Fig. 4a shows the HAADF-STEM image for the $CoFe_2O_4$/graphene hybrids. The $CoFe_2O_4$ nanocrystals were very tiny and anchored on the surface of graphene, forming honeycomb and sandwich-like structures. Fig. 4b displays the EDX spectrum of the $CoFe_2O_4$/graphene hybrids. The spectrum demonstrates the existence of carbon, oxygen, iron and cobalt in the samples, which is coincident with the XRD results. Moreover, quantitative

analysis of the EDX spectrum indicates that the atomic ratio of Co:Fe is nearly 1:2, inferring a $CoFe_2O_4$ composition. Fig. 4c-f shows the corresponding EDX elemental mapping of C (K_α, 0.28 keV), O (K_α, 0.52 keV), Fe (K_α, 6.4 keV) and Co (K_α, 6.9 keV). It is clear that the elements C (Fig. 4c), O (Fig. 4d), Fe (Fig. 4e) and Co (Fig. 4f) is evenly distributed throughout the whole HAADF-STEM image perturbed only by a thickness contrast, which suggests that tiny $CoFe_2O_4$ nanocrystals covered on the graphene nanosheets and form Sandwich-like structures. This result is accordant with the above TEM observations.

Fig. 5 shows the magnetization versus magnetic field (*M-H*) curve of the pure $CoFe_2O_4$ nanocrystals and $CoFe_2O_4$/graphene hybrids measured at room temperature. The saturation magnetization (M_s) value of the pure $CoFe_2O_4$ nanocrystals and $CoFe_2O_4$/graphene hybrids is 63.8 and 45.3 emu/g, respectively, which is smaller than that of the corresponding bulk $CoFe_2O_4$ (74 emu/g). These results are ascribed to the possible effect of surface spin canting and/or dead magnetic layer on the $CoFe_2O_4$ nanocrystals.[34] Morover, the smaller M_s of the $CoFe_2O_4$/graphene hybrids in respect to the pure $CoFe_2O_4$ nanocrystals is originated from the weight-fraction of non-magnetic graphene. Both of the samples show S-like shape with zero coercivity and remanence, demonstrating a typical superparamagnetic characteristic which is favorable for their usage as high-performance electromagnetic wave absorbers working at high frequency range.

Fig. 6 shows the frequency dependence of complex permeability and complex permittivity for the pure $CoFe_2O_4$ nanocrystals and $CoFe_2O_4$/graphene hybrids. No

significant changes of the complex permeability are observed between the pure $CoFe_2O_4$ nanocrystals and $CoFe_2O_4$/graphene hybrids (Fig. 6a). The real part (μ') of complex permeability for both the samples presents a similar frequency dependence and the values decrease slowly with the increase of frequency. It is clearly seen that the μ' value of $CoFe_2O_4$/graphene hybrids is slightly decreased in comparison with the pure $CoFe_2O_4$ nanocrystals. This phenomenon is mainly attributed to the additional nonmagnetic GO in the hybrids. The imaginary part (μ'') of complex permeability is almost the same, suggesting a negligible difference of magnetic loss between both the samples. The resonance peak around 12 GHz is possibly ascribed to exchange resonance of the magnetic nanocrystals.[35] The real part (ε') and imaginary part (ε'') of complex permittivity for the pure $CoFe_2O_4$ nanocrystals (Fig. 6b) are almost independent on frequency, which are nearly constant in the whole frequency range with an inconspicuous undulation ($\varepsilon' \approx 4.6$ and $\varepsilon'' \approx 0.33$). For the $CoFe_2O_4$/graphene hybrids, the complex permittivity is obviously enhanced and decline with the increase of frequency. The values of ε' and ε'' declines from 18.6 to 4.5 and 6.7 to 1.3, respectively, 3.5 and 24.7 times larger than that of the pure $CoFe_2O_4$ nanocrystals at 0.1 GHz. This result is attributed to the enhanced electric polarization and electrical conductivity by additional graphene, which could lead to enhanced dielectric dispersion and increased dielectric loss in comparison with the pure $CoFe_2O_4$ nanocrystals. In addition, the fluctuation of complex permittivity about 10 GHz for the $CoFe_2O_4$/graphene hybrids is probably due to the dipolar polarization dominated in the insulator-conductor composites.[35]

Fig. 7 shows the frequency dependence of dissipation factors represented by the magnetic loss tangent ($\tan\delta_\mu = \mu''/\mu'$) and dielectric loss tangent ($\tan\delta_\varepsilon = \varepsilon''/\varepsilon'$) for the pure $CoFe_2O_4$ nanocrystals and $CoFe_2O_4$/graphene hybrids. The values of $\tan\delta_\mu$ and $\tan\delta_\varepsilon$ for the pure $CoFe_2O_4$ nanocrystals are smaller than 0.2 in the whole frequency range, indicating that the magnetic loss and dielectric loss are considerably lower, which suggests that the pure $CoFe_2O_4$ nanocrystals may represent poor electromagnetic wave absorption properties. It is clear that the values of $\tan\delta_\varepsilon$ for the $CoFe_2O_4$/graphene hybrids are obviously enhanced in comparison with that of the pure $CoFe_2O_4$ nanocrystals. This result indicate that the lightweight graphene play an important role to increase the dielectric loss, which is significant for the electromagnetic wave absorption. Besides, the reduction process of GO in this work may generate lots of defect sits in the 2D lattice of graphene, which can lead to an increase in the complex permittivity and enhance the dielectric loss of the electromagnetic wave absorption materials.[36] Moreover, the values of $\tan\delta_\varepsilon$ are distinctly larger than that of the $\tan\delta_\mu$, suggesting that the electromagnetic wave attenuation mechanism of the $CoFe_2O_4$/graphene hybrids is mainly attributed to the dielectric loss.

To further investigate the electromagnetic wave absorption properties of $CoFe_2O_4$/graphene hybrids, the reflection loss (RL) curves were calculated according the transmit line theory by the following equations:[5]

$$RL = 20\log\left|\frac{Z_{in} - Z_0}{Z_{in} + Z_0}\right| \qquad (1)$$

$$Z_{in} = Z_0 \left(\mu_r / \varepsilon_r\right)^{1/2} \tanh\left\{ j\left(2\pi fd / c\right)\left(\mu_r \varepsilon_r\right)^{1/2} \right\} \qquad (2)$$

where Z_{in} is the input impendence of absorber, Z_0 is the impedance of air, f is the frequency of electromagnetic wave, d is the thickness of a electromagnetic wave absorber and c is the velocity of light in vacuum. Fig. 8 display the relationship between RL and frequency for the pure $CoFe_2O_4$ nanocrystals and $CoFe_2O_4$/graphene hybrids. The RL values for the pure $CoFe_2O_4$ nanocrystals (Fig. 8a) cannot reach -10 dB with the thickness range of 1.0-4.0 mm and the maximum RL value is only -4.4 dB, revealing weak electromagnetic wave absorption ability. However, when the superparamagnetic $CoFe_2O_4$ nanocrystals are anchored on the graphene nanosheets, the electromagnetic wave absorption properties of $CoFe_2O_4$/graphene hybrids are obviously enhanced. The RL value of $CoFe_2O_4$/graphene hybrids (Fig. 8b) below -10 dB can be achieved in the 5.4-18 GHz range with the thickness of 1.5-4.0 mm, and the maximum RL value of -36.4 dB can be obtained at 12.9 GHz with a matching thickness of only 2.5 mm. It is clear that the graphene nanosheets are significantly important for the electromagnetic wave absorption properties of $CoFe_2O_4$/graphene hybrids. In comparison with the pure graphene and $CoFe_2O_4$ nanocrystals, the enhanced electromagnetic wave absorption performance of $CoFe_2O_4$/graphene hybrids is ascribed to the synergistic effect between superparamagnetic $CoFe_2O_4$ nanocrystals and light-weight graphene. Accompanying with the low density of graphene, these results suggest that the $CoFe_2O_4$/graphene hybrids are promised to be used as light weight and high-performance electromagnetic wave absorber for electromagnetic wave absorption applications in the future.

4. Conclusion

In summary, we developed a facile one-pot polyol strategy to fabricate sandwich-structured graphene nanosheets decorated by superparamagnetic $CoFe_2O_4$ nanocrystals, and their nanostructures and morphologies were characterized at nanoscale. Electromagnetic wave absorption properties show that the maximum RL of superparamagnetic $CoFe_2O_4$/graphene hybrids is -36.4 dB at 12.9 GHz for the thickness of 2.5 mm and the absorption bandwidth with the RL below -10 dB is 12.6 GHz (5.4-18 GHz) for the thickness of 1.5-4.0 mm. Investigations reveal that the introduction of graphene could significantly enhance electromagnetic wave absorption properties of the $CoFe_2O_4$ nanocrystals. The enhanced electromagnetic wave absorption performance of superparamagnetic $CoFe_2O_4$/graphene hybrids is ascribed to the synergistic effect between remarkable magnetic loss from the superparamagnetic $CoFe_2O_4$ nanocrystals and high electric loss from the light-weight graphene. This work suggests that the sandwich-like $CoFe_2O_4$/graphene hybrids may be attractive candidate for light weight and enhanced electromagnetic wave absorption applications in the future.

Acknowledgments

We thank the support from the grants from the National Natural Science Foundation of China (No. 61177059), Introduction Talent Project of Northwest University (pr13100), the Natural Science Foundation of Shannxi Province,China (2014JQ1040), the Scientific Research Foundation of Northwest University (13NW13), the Basic Scientific Research Business Expenses of the Central University, Open Project of Key

Laboratory for Magnetism and Magnetic Materials of the Ministry of Education from Lanzhou University and the Open Projects from Institute of Photonics and Photo-Technology of Northwest University (China).

References

[1] J. W. Liu, R. C. Che, H. J. Chen, F. Zhang, F. Xia, Q. S. Wu and M. Wang, *Small*, 2012, **8**, 1214.

[2] A. M. Wang, W. Wang, C. Long, W. Li, J. G. Guan, H. S. Gu and G. X. Xu, J. Mater. Chem. C, 2014, **2**, 3769.

[3] Y. Li, J. Zhang, Z. W. Liu, M. M. Liu, H. J. Lin and R. C. Che, *J. Mater. Chem. C*, 2014, **2**, 5216.

[4] X. Sun, J. P. He, G. X. Li, J. Tang, T. Wang, Y. X. Guo, H. R. Xue, *J. Mater. Chem. C*, 2013, **1**, 765.

[5] X. H. Li, H. B. Yi, J. W. Zhang, J. Feng, F. S. Li, D. S. Xue, H. L. Zhang, Y. Peng and N. J. Mellors, *J. Nanopart. Res.*, 2013, **15**, 1472.

[6] C. L. Zhu, M. L. Zhang, Y. J. Qiao, G. Xiao, F. Zhang and Y. J. Chen, *J. Phys. Chem. C*, 2010, **114**, 16229.

[7] F. L. Wang, J. R. Liu, J. Kong, Z. J. Zhang, X. Z. Wang, M. Itoh and K. I. Machida, *J. Mater. Chem.*, 2011, **21**, 4314.

[8] J. W. Zhang, C. Yan, S. J. Liu, H. S. Pan, C. H. Gong, L. G. Yu and Z. J. Zhang, *Appl. Phys. Lett.*, 2012, **100**, 233104.

[9] F. Xia, J. W. Liu, D. Gu, P. F. Zhao, J. Zhang and R. C. Che, *Nanoscale*, 2011, **3**, 3860.

[10] A. Ohlan, K. Singh, A. Chandra and S. K. Dhawan, *ACS Appl. Mater. Interfaces*, 2010, **2**, 927.

[11] V. Georgakilas, M. Otyepka, A. B. Bourlinos, V. Chandra, N. Kim, K. C. Kemp, P. Hobza, R. Zboril and K. S. Kim, *Chem. Rev.*, 2012, **112**, 6156.

[12] C. Wang, X. J. Han, P. Xu, X. L. Zhang, Y. C. Du, S. R. Hu, J. Y. Wang and X. H. Wang, *Appl. Phys. Lett.*, 2011, **98**, 072906.

[13] W. I. Park, C. H. Lee, J. M. Lee, N. J. Kim and G. C. Yi, *Nanoscale*, 2011, **3**, 3522.

[14] S. Bai and X. P. Shen, *RSC Adv.*, 2012, **2**, 64.

[15] Y. Huang, J. J. Liang and Y. S. Chen, *Small*, 2012, **8**, 1805.

[16] X. Huang, Z. Y. Yin, S. X. Wu, X. Y. Qi, Q. Y. He, Q. C. Zhang, Q. Y. Yan, F. Boey and H. Zhang, *Small*, 2011, **7**, 1876.

[17] M. Fu, Q. Z. Jiao, Y. Zhao, *J. Mater. Chem. A,* 2013, **1**, 5577.

[18] M. Zong, Y. Huang, X. Ding, N. Zhang, C. H. Qu and Y. L. Wang, *Ceram. Int.*, 2014, **40**, 6821.

[19] G. S. Wang, Y. Wu, Y. Z. Wei, X. J. Zhang, Y. Li, L. L. Li, B. Wen, P. G. Yin, L. Guo, M. S. Cao, *ChemPlusChem,* 2014, **79**, 375.

[20] P. B. Liu and Y. Huang, *RSC Adv.*, 2013, **3**, 19033.

21 X. C. Zhao, Z. M. Zhang, L. Y. Wang, K. Xi, Q. Q. Cao, D. H. Wang, Y. Yang and Y. W. Du, *Scientific Reports*, 2013, **3**, 3421.

[22] Y. J. Chen, Z. Y. Lei, H. Y. Wu, C. L. Zhu, P. Gao, Q. Y. Ouyang, L. H. Qi and W. Qin, *Mater. Res. Bull.*, 2013, **48**, 3362.

[23] T. T. Chen, F. Deng, J. Zhu, C. F. Chen, G. B. Sun, S. L. Ma and X. J. Yang, *J.*

Mater. Chem., 2012, **22**, 15190.

[24] D. Z. Chen, G. S. Wang, S. He, J. Liu, L. Guo and M. S. Cao, *J. Mater. Chem. A*, 2013, **1**, 5996.

[25] R. C. Che, C. Y. Zhi, C. Y. Liang and X. G. Zhou, *Appl. Phys. Lett.*, 2006, **88**, 033105.

[26] J. Cao, W. Y. Fu, H. B. Yang, Q. J. Yu, Y. Y. Zhang, S. K. Liu, P. Sun, X. M. Zhou, Y. Leng, S. M. Wang, B. B. Liu and G. T. Zou, *J. Phys. Chem. B*, 2009, **113**, 4642.

[27] N. Gandhi, K. Singh, A. Ohlan, D. P. Singh and S. K. Dhawan, *Compos. Sci. Technol.*, 2011, **71**, 1754.

[28] M. Fu, Q. Z. Jiao, Y. Zhao and H. S. Li, *J. Mater. Chem. A*, 2014, **2**, 735.

[29] M. Zong, Y. Huang, H. W. Wu, Y. Zhao, Q. F. Wang and X. Sun, *Mater. Lett.*, 2014, **114**, 52.

[30] W. S. Hummers and R. E. Offeman, *J. Am. Chem. Soc.*, 1958, **80**, 1339.

[31] X. H. Li, H. Zhu, J. Feng, J. W. Zhang, X. Deng, B. F. Zhou, H. L. Zhang, D. S. Xue, F. S. Li, N. J. Mellors, Y. F. Li and Y. Peng, *Carbon*, 2013, **60**, 488.

[32] M. Zong, Y. Huang, Y. Zhao, X. Sun, C. H. Qu, D. D. Luo and J. B. Zheng, *RSC Adv.*, 2013, **3**, 23638.

[33] J. C. González, J. C. Hernández, M. López-Haro, E. del Río, J. J. Delgado, A. B. Hungría, S. Trasobares, S. Bernal, P. A. Midgley and J. J. Calvino, *Angew. Chem. Int. Ed.*, 2009, **48**, 5313.

[34] X. H. Li, C. L. Xu, X. H. Han, L. Qiao, T. Wang and F. S. Li, *Nanoscale Res. Lett.*, 2010, **5**, 1039.

[35] F. Ma, Y. Qin, Y. Z. Li, *Appl. Phys. Lett.*, 2010, **96**, 202507.

[36] D. D. Zhang, D. L. Zhao, J. M. Zhang and L. Z. Bai, *J. Alloys Compd.*, 2014, **589**, 378.

Figure Caption

Fig. 1 XRD patterns of GO and $CoFe_2O_4$/graphene hybrids

Fig. 2 TEM images of (a, b) GO and (c-f) $CoFe_2O_4$/graphene hybrids. Inset of Fig. 2a and c show the SAED patterns of GO and $CoFe_2O_4$/graphene hybrids, respectively; Inset of Fig. 2b and d show the HRTEM images of GO and $CoFe_2O_4$/graphene hybrids, respectively.

Fig. 3 XPS spectra: (a) wide scan of GO and $CoFe_2O_4$/graphene hybrids, (b) O1s spectra of GO and $CoFe_2O_4$/graphene hybrids, (c) Fe2p spectra of $CoFe_2O_4$/graphene hybrids, (d) Co2p spectra of $CoFe_2O_4$/graphene hybrids, (e) C1s spectra of GO and (f) C1s spectra of $CoFe_2O_4$/graphene hybrids

Fig. 4 Elemental mappings of $CoFe_2O_4$/graphene hybrids: (a) HAADF-STEM image; (b) EDX spectrum; (c) carbon mapping; (d) oxygen mapping; (e) iron mapping; (f) cobalt mapping.

Fig. 5 The *M-H* curve of the samples measured at room temperature.

Fig. 6 The frequency dependence of (a) complex permeability and (b) complex permittivity for the pure $CoFe_2O_4$ nanocrystals and $CoFe_2O_4$/graphene hybrids

Fig. 7 Frequency dependence of the loss tangent of (a) pure $CoFe_2O_4$ nanocrystals and (b) $CoFe_2O_4$/graphene hybrids

Fig. 8 The relationship between RL and frequency for the (a) pure $CoFe_2O_4$ nanocrystals and (b) $CoFe_2O_4$/graphene hybrids

Table Caption

Table 1 The peak area ratios of the carbon-based groups for GO and $CoFe_2O_4$/graphene hybrids

Fig. 1

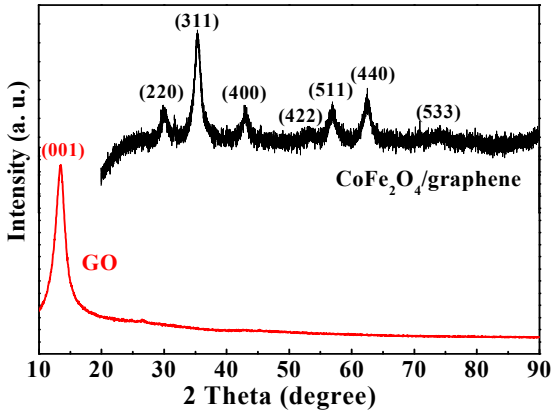

Fig. 2

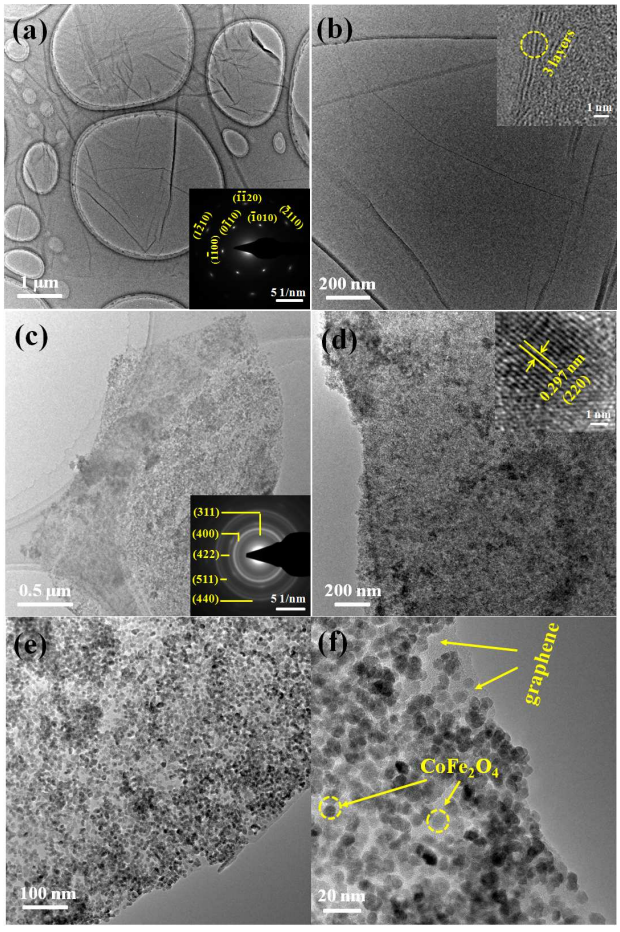

Fig. 3

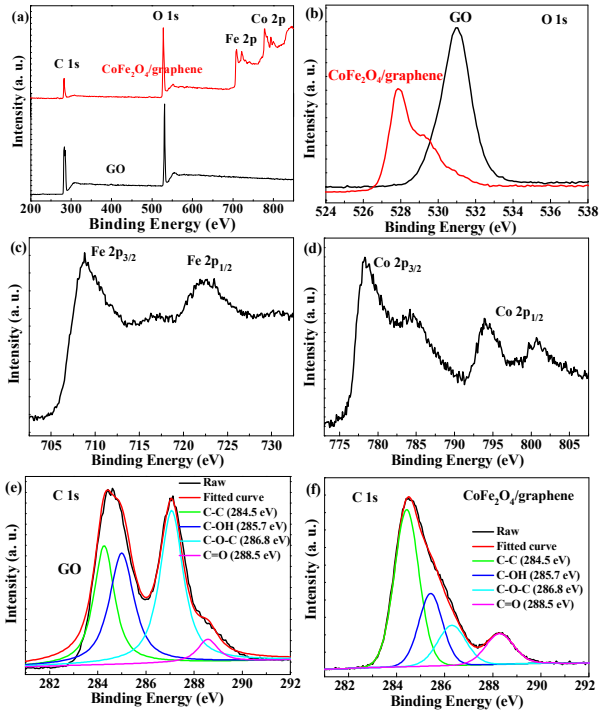

Fig. 4

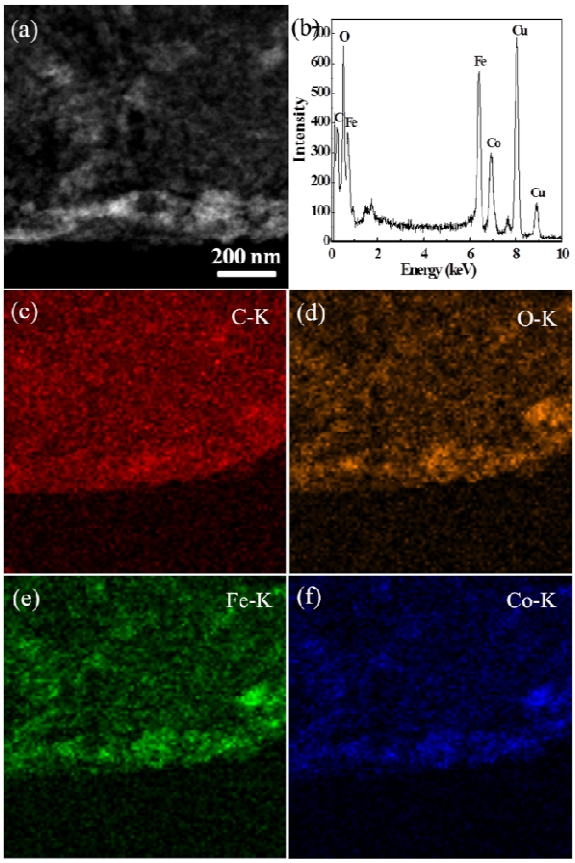

Fig. 5

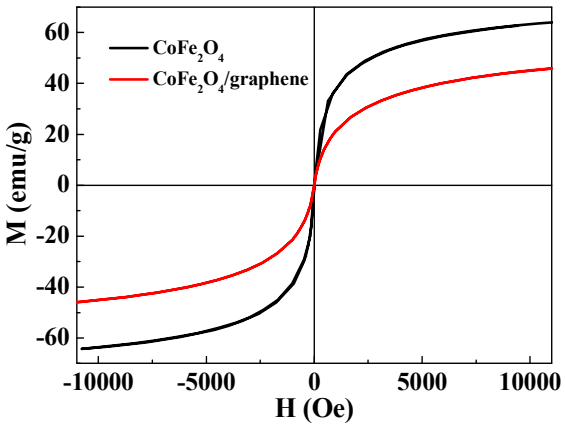

Fig. 6

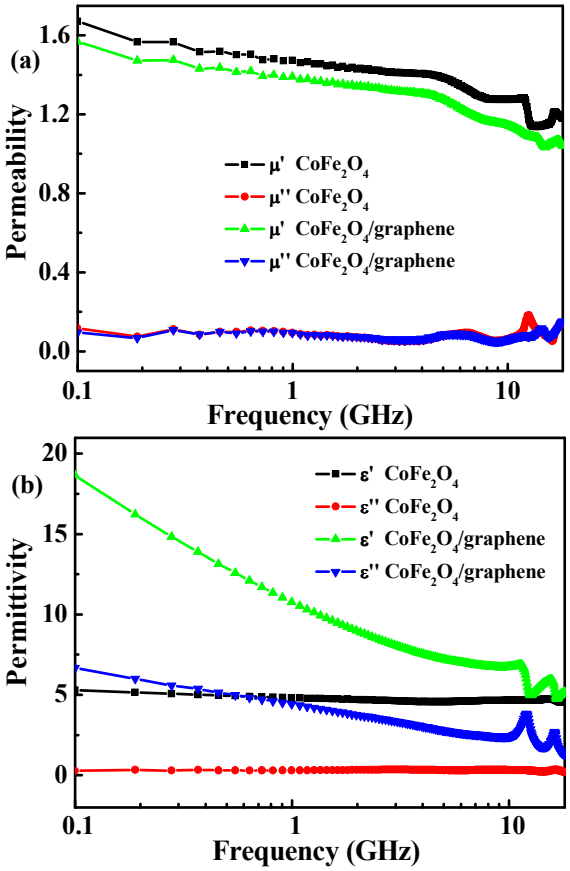

Fig. 7

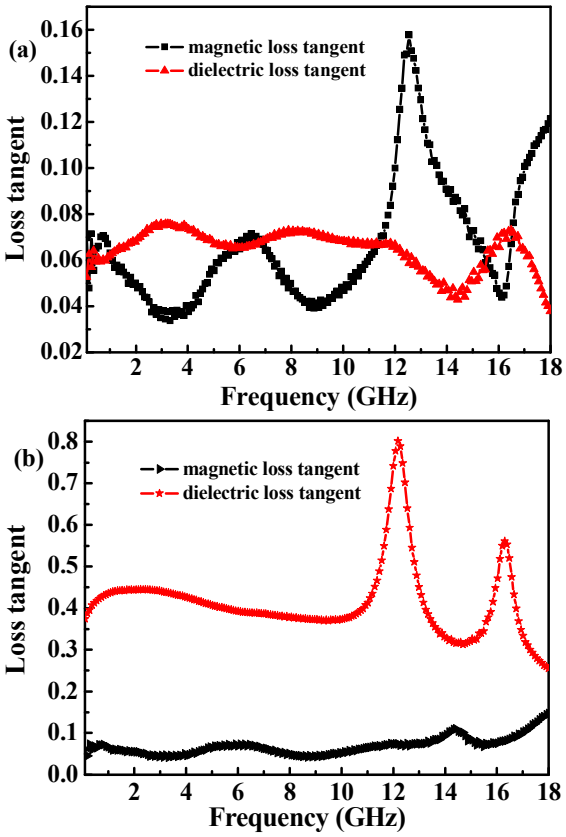

Fig. 8

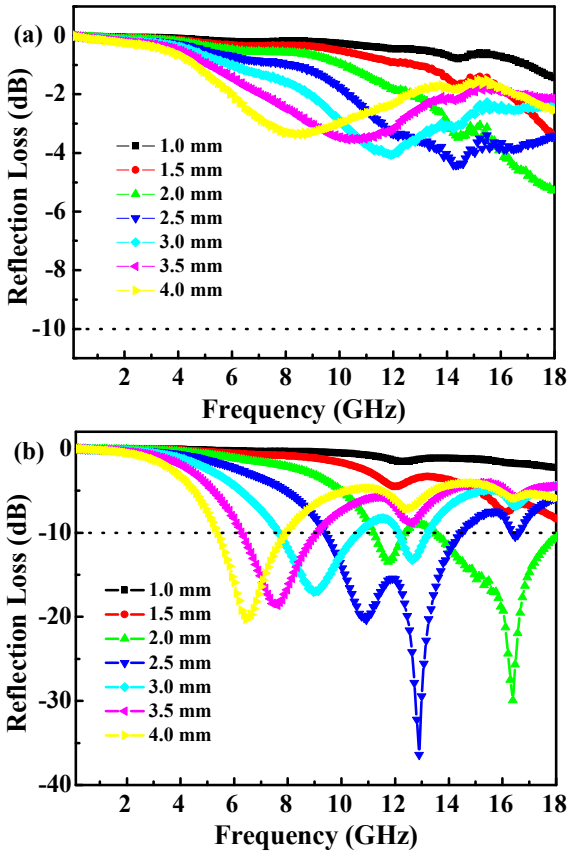

Table 1

Chemical Band	C-C	C-OH	C-O-C	C=O
Binding Energy (eV)	285.0	286.1	287.1	288.9
Relative area of GO (%)	45.2	10.1	36.0	8.7
Relative area of $CoFe_2O_4$/graphene hybrids (%)	57.0	29.7	13.3	0